

# Synthesis, Characterization, and Metal Ions Adsorption Properties of Chitosan–Calixarenes ( I )

Hai-Bing Li, Yuan-Yin Chen, Shi-Lan Liu

Department of Chemistry, Wuhan University, 430072 Wuhan, China

Received 7 May 2002; accepted 13 September 2002

**ABSTRACT:** Calixarene-modified chitosans (CTS–CA-I and CTS–CA-II) were first synthesized by the reaction of chitosan (CTS–NH<sub>2</sub>) with 1,3-bis-chloroethoxyethoxy-2,4-dihydroxy-*p*-*tert*-butylcalix[4]arene (CA-I) or its benzoyl derivative (CA-II). Their structures were characterized by infrared and X-ray diffraction spectroscopy and scanning electron microscopy (SEM). The adsorption of Ni<sup>2+</sup>, Cd<sup>2+</sup>, Cu<sup>2+</sup>, Pd<sup>2+</sup>, Ag<sup>+</sup>, and Hg<sup>2+</sup> by CTS–CA-I and CTS–CA-II was studied and the thermodynamic parameter of two calix-

arene-modified chitosans toward Hg<sup>2+</sup> was deduced. The adsorption properties of CTS–CA-I and CTS–CA-II were greatly varied compared with that CTS–NH<sub>2</sub>, especially with the adsorption capacity toward Ag<sup>+</sup> and Hg<sup>2+</sup>, because of the presence of the calixarene moiety. © 2003 Wiley Periodicals, Inc. *J Appl Polym Sci* 89: 1139–1144, 2003

**Key words:** modification; adsorption; resins

## INTRODUCTION

Chitin is one of the most abundant organic materials that can be easily obtained in nature. By *N*-deacetylation, chitin can be easily degraded to chitosan (CTS), a nitrogenous polysaccharide composed mainly of  $\beta$ -(1-4)-2-amino-2-deoxy-D-glucopyranose repeating units. Because of its specific structures and properties, CTS has recently drawn great attention for its industrial and medical applications, such as use an artificial skin and to capture metal from waste water.<sup>1–4</sup> Furthermore, the free primary amino groups and hydroxyl groups at the sixth position in the pyranose ring of CTS enable a variety of chemical modifications. A series of hyperbranched CTS derivatives has been synthesized.<sup>5</sup> Crowns have been successfully incorporated into the matrix of CTS.<sup>6</sup> An  $\alpha$ -cyclodextrin (CD)-linked CTS derivative has been prepared via a reductive amination strategy.<sup>7</sup> A  $\beta$ -CD-modified *N*-carboxymethylchitosan has been synthesized as a chiral high-performance liquid chromatography (HPLC) stationary phase.<sup>8</sup>

On the other hand, calixarenes (Figure 1), a family of cavity-shaped cyclic molecules obtained from formaldehyde and *para*-substituted phenols via ring-closing condensation under alkaline conditions, have also attracted much attention.<sup>9</sup> Calixarenes have demonstrated outstanding complex ability towards ions, organic molecules, etc., and are considered the third best

host molecules, after crowns and CDs.<sup>9–11</sup> It is interesting to see what happens when these two kinds of molecules are combined. To the best of our knowledge, no report concerning this topic has been published to date. Here we present the first report on the synthesis, characterization, and adsorption properties towards Ni<sup>2+</sup>, Cd<sup>2+</sup>, Cu<sup>2+</sup>, Pd<sup>2+</sup>, Ag<sup>+</sup>, and Hg<sup>2+</sup> of calixarene-modified CTS.

## EXPERIMENTAL

### Materials

Chitosan (CTS) was prepared by *N*-deacetylation of chitin from shrimp shells. Its degree of deacetylation was calculated from the nitrogen content as 80%. All solvents were purified by standard procedures. Petroleum ether refers to the fraction with a boiling point in the range 60–90°C. All other chemicals were analytically pure and used without further purification.

### Measurements

Infrared (IR) spectra were measured on a Nicolet 5DX FT-IR spectrophotometer, and wide-angle X-ray diffraction (WAXD) patterns were recorded with a film camera using nickel-filtered Cu-K $\alpha$  radiation produced by a Rigaku (D/MAX, 111A) diffractometer. Melting points (mp) were recorded on a Gallenkamp mp apparatus in open capillaries and are uncorrected. The morphology of film surfaces, after the surfaces were coated with gold, was examined by scanning electron microscopy (SEM; SX-650, Hitachi, Japan) at an accelerating voltage of 25 kV. Proton nuclear mag-

Correspondence to: Y. Chen (yychen@whu.edu.cn)

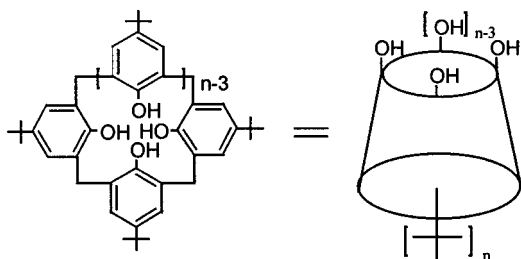


Figure 1 Structure of calixarenes.

netic resonance ( $^1\text{H}$  NMR) spectra were recorded on Varian Mercury VX300 instruments at ambient temperature. Tetramethylsilane (TMS) was used as an internal standard. Fast atom bombardment mass spectroscopy (FABMS) spectra, with *m*-nitrobenzyl alcohol as a matrix, were obtained from a Kratos MS80RF mass spectrometry service. Elemental analyses were performed by the Analytical Laboratory of the Department of Chemistry at Wuhan University (results are shown in Table I).

#### Synthesis of CA-I (5,11,17,23-tetra-*tert*-butyl-25,27-bis[2'-( $\beta$ -chloroethoxy)ethoxy]-26,28-dihydroxycalix[4]arene)

A suspension of *p*-*tert*-butylcalix[4]arene (1.48 g, 2.0 mmol),  $\text{K}_2\text{CO}_3$  (0.41 g, 3.0 mmol), and 2-( $\beta$ -chloroethoxy)ethyltosylate (1.34 g, 4.8 mmol) in dry  $\text{CH}_3\text{CN}$  (60 mL) was refluxed for 24 h. The reaction mixture was cooled, and the solvent was removed under reduced pressure. The solid residue was then dissolved in  $\text{CH}_2\text{Cl}_2$ , and undissolved residue was filtered. The filtrate was evaporated under reduced pressure, and the residue was recrystallized from  $\text{CH}_3\text{CN}$  to give CA-I. Yield: 78.2%; mp: 178–180°C ( $\text{CH}_2\text{Cl}_2/\text{MeOH}$ ). FABMS: *m/e*: 860 ( $\text{M}^+$ ).  $^1\text{H}$  NMR ( $\delta$ , ppm): 7.01 (4H, s, ArH), 6.96 (2H, s, ArOH), 6.72 (4H, s, ArH), 4.50 and 3.30 (8H, d, ABq,  $J = 13.6$  Hz,  $\text{ArCH}_2\text{Ar}$ ), 4.01 (12H, m,  $\text{OCH}_2$ ), 3.72 (4H, t,  $J = 6.3$  Hz,  $\text{CH}_2\text{Cl}$ ), 1.30 (18H, s, t-Bu), 0.92 (18H, s, t-Bu).

ANAL. Calcd for  $\text{C}_{52}\text{H}_{70}\text{O}_6\text{Cl}_2$ : C, 85.71%; H, 6.12%. Found: C, 85.25%; H, 6.15%.

#### Synthesis of CA-II (5,11,17,23-tetra-*tert*-butyl-25,27-bis[2'-( $\beta$ -chloroethoxy)ethoxy]-26,28-dibenzoylcalix[4]arene)

CA-II was obtained by reacting CA-I with BzBr in the presence of NaH as a base. The product was recrystallized from  $\text{CH}_2\text{Cl}_2/\text{MeOH}$ . Yield: 62%; mp: 193–194°C. FABMS: *m/e*: 1041 ( $\text{M}^+$ ).  $^1\text{H}$  NMR (see Figure 2) ( $\delta$ , ppm): 7.29 (10H, m, ArH), 6.95 (4H, s, ArH), 6.40 (4H, s, ArH), 4.59 (s, 4H,  $\text{OCH}_2\text{Ar}$ ), 4.25 and 3.02 (8H, d, ABq,  $J = 12.6$  Hz,  $\text{ArCH}_2\text{Ar}$ ), 3.98 (4H, t,

$\text{OCH}_2\text{CH}_2$ ), 3.62 (4H, t,  $\text{OCH}_2\text{CH}_2$ ), 3.18 (4H, t,  $\text{OCH}_2\text{CH}_2\text{Cl}$ ), 3.10 (4H, t,  $\text{OCH}_2\text{CH}_2$ ), 1.22 (18H, s, t-Bu), 0.83 (18H, s, t-Bu).

ANAL. Calcd for  $\text{C}_{66}\text{H}_{82}\text{O}_6\text{Cl}_2$ : C, 76.06%; H, 7.93%. Found: C, 76.15%; H, 8.05%.

#### Synthesis of calix[4]arene-crosslinked chitosans

The synthetic route of CTS-CA is shown in Figure 3. CTS is a linear polymer with both hydroxyl and amino groups. Three modes for the crosslinking reactions are possible: (I) a reaction between amino and hydroxyl groups, (II) a reaction between two amino groups, and (III) a reaction between two hydroxyl groups.

A  $\text{CH}_3\text{CN}$  (20 mL) solution of CA-I (0.5 g) was dropped slowly into a mixture of  $\text{K}_2\text{CO}_3$  (1.0 g), KOH (0.2 g), and a suspension of swelled CTS- $\text{NH}_2$  in 40 mL of ethanol under a nitrogen atmosphere and with stirring. The mixture was refluxed with good agitation for 24 h, filtered, extracted thoroughly by a Soxhlet's extractor with  $\text{CHCl}_3$  to remove any unreacted CA-I, and dried to yield 1.2 g of CTS-CA-I as a light yellow powder.

The polymer CTS-CA-II was prepared from CTS- $\text{NH}_2$  and CA-II using the same procedure as described for the preparation of CTS-CA-I. The product was obtained in 74% yield.

#### Ability to absorb metal ions of CTS-CA

To twenty-five milliliters of a known concentration of an aqueous solution of salt picrate was added 25 mg of CTS-CA sample. After stirring for 12 h at room temperature, the mixture was centrifuged and filtered. The picrate concentration in the filtrate was determined by ultraviolet (UV) spectra, and the quantity of metal ion absorbed by CTS-CA was calculated as follows:

$$Q = \frac{V(C_0 - C)M_{\text{cation}}}{nW} \quad (1)$$

where  $Q$  is the adsorption capacities of CTS derivatives (mg metal ion/g adsorbent),  $V$  is the volume of metal ion solution (mL),  $C_0$  is the concentration of picrate before adsorption ( $\text{mmol mL}^{-1}$ ),  $C$  is the con-

TABLE I  
Elemental Analysis Results of CTS-CA

Chitosan	C%	H%	N%
CTS- $\text{NH}_2$	38.58	6.98	6.95
CTS-CA-I	46.47	6.25	4.36
CTS-CA-II	49.91	6.61	4.18

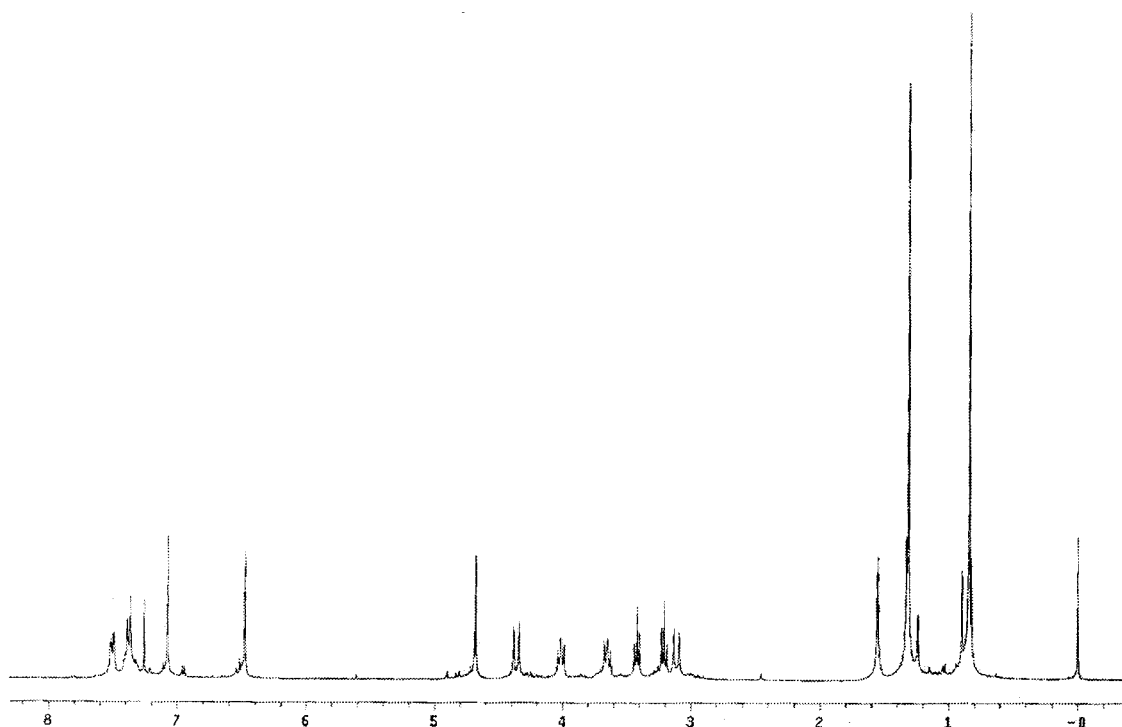


Figure 2 <sup>1</sup>H NMR spectrum of CA-II.

centration of picrate after adsorption ( $\text{mmol mL}^{-1}$ ),  $n$  is the valence of metal ion, and  $W$  is the weight of CTS-CA (g).

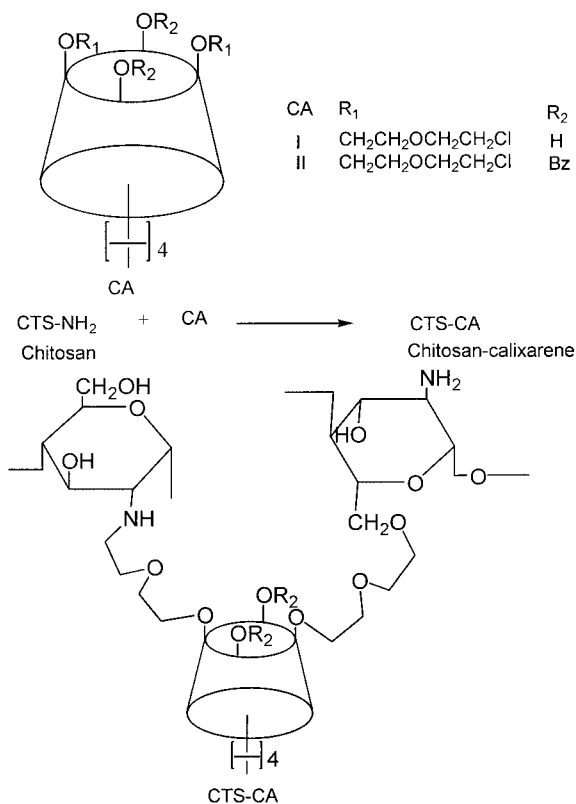


Figure 3 Reaction scheme for the synthesis of CTS-CA.

RESULTS AND DISCUSSION

Characterization of structure of CTS-CA

CTS-CA was successfully prepared by the reaction between —NH<sub>2</sub> and/or —OH on the C<sub>6</sub> in CTS and —CH<sub>2</sub>Cl in calixarenes. CTS-CA was light yellow in color and did not dissolve in solvents such as chloroform, dimethyl sulfoxide (DMSO), and dimethylform-

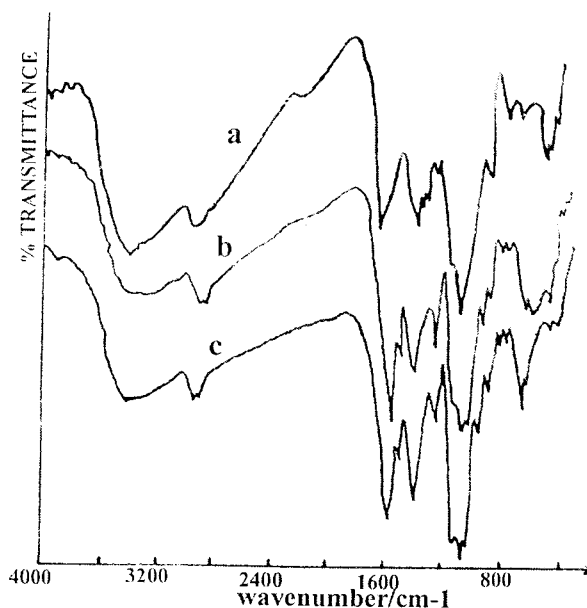
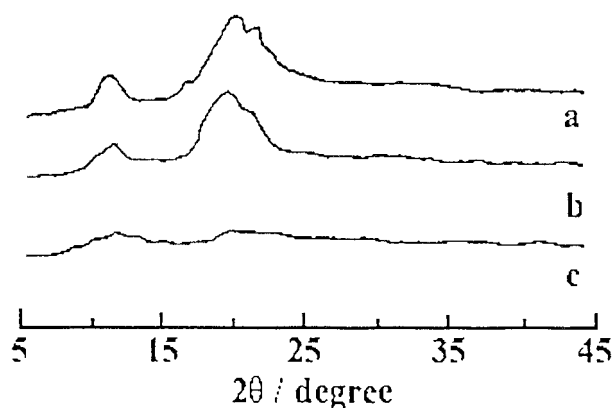


Figure 4 Infrared spectra of (a) CTS-NH<sub>2</sub>, (b) CTS-CA-I, and (c) CTS-CA-II.



**Figure 5** X-ray diffraction patterns of (a) CTS-NH<sub>2</sub>, (b) CTS-CA-I, and (c) CTS-CA-II.

amide (DMF), etc. CTS-CA samples were swollen in acetic acid solution.

#### Infrared spectral analysis

The Fourier transform infrared (FTIR) spectra of CTS-CA-I and CTS-CA-II are shown together with that of CTS-NH<sub>2</sub> in Figure 4. Although marked difference were not observed in the FTIR spectra, the characteristic peaks of aromatic backbone vibration appeared at 1540 and 1521 cm<sup>-1</sup> and the characteristic peak of aromatic C—H in the out-of-plane deformation appeared at 932 and 743 cm<sup>-1</sup> because of the presence of phenyl groups. It was also seen that CTS and its derivatives have the characteristic peak at 900 cm<sup>-1</sup> caused by the pyranil group in the CTS backbone.

#### X-ray diffraction analysis

The WAXD patterns of CTS-CA-I and CTS-CA-II are shown together with that of CTS-NH<sub>2</sub> in Figure 5. The WAXD pattern of CTS-NH<sub>2</sub> showed the characteristic peaks at 2θ = 10 and 20°. It was noted that the peaks at 2θ = 10° and 20° decreased greatly in CTS-CA-I and

**TABLE II**  
Ability of CTS-CA to Absorb Metal Ions<sup>a</sup>

Metal ion	pH	CTS-CA-I	CTS-CA-II	CTS-NH <sub>2</sub>
Ni <sup>2+</sup>	5.0	35.9	35.4	45.9
Cd <sup>2+</sup>	5.5	15.2	17.4	35.2
Cu <sup>2+</sup>	5.6	18.9	18.3	63.4
Pd <sup>2+</sup>	2.0	65.3	79.1	99.8
Ag <sup>+</sup>	5.3	74.6	87.8	105.2
Hg <sup>2+</sup>	5.0	19.4	25.9	88.0

<sup>a</sup> Values expressed as mg metal ion/g adsorbent.

CTS-CA-II. It was thought that the decrease in crystallinity of CTS-CA was attributed to the deformation of the strong hydrogen bond in the CTS-NH<sub>2</sub> backbone at the amino groups or hydroxyl were substituted by calixarenes. The two CTS derivatives have a low crystallinity, indicating that they are considerably more amorphous than CTS-NH<sub>2</sub>.

#### SEM characterization

SEMs of the surface morphology of CTS and its derivatives are presented in Figure 6. CTS has a smooth surface (Fig. 6a), whereas CTS-CA-I exhibits a porous surface structure (Fig. 6b) that is caused by the removal by extraction of the soluble linear polymer from the crosslinked CTS-CA-I. In contrast, the surface of CTS-CA-II does not exhibit the same structure as CTS-CA-I (Fig. 6c). This difference may be attributed to the higher crosslinked density of CTS-CA-II than of CTS-CA-I.

#### Evaluation of CTS-CA as adsorbents for metal ions

Adsorption capacity experimental results of CTS-CA

The adsorption experimental results of CTS-CA for Ni<sup>2+</sup>, Cd<sup>2+</sup>, Cu<sup>2+</sup>, Pd<sup>2+</sup>, Ag<sup>+</sup>, and Hg<sup>2+</sup> are shown together with those of CTS-NH<sub>2</sub> in Table II. These results indicate that the adsorption capacity of CTS-CA

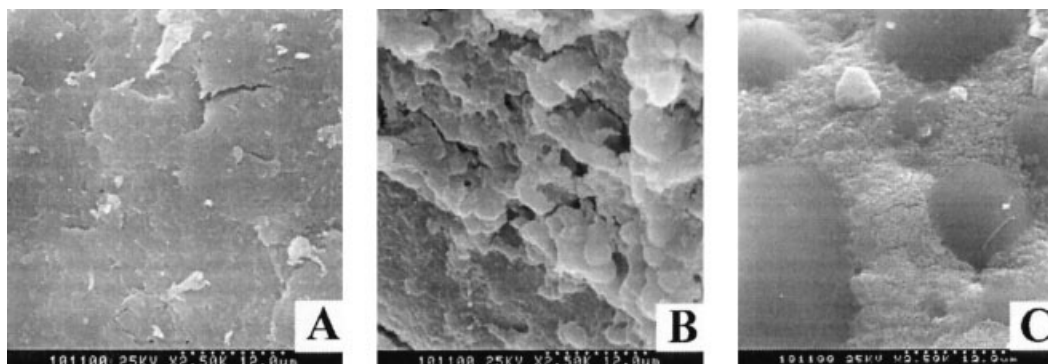


**Figure 6** SEM of (A) CTS-NH<sub>2</sub>, (B) CTS-CA-I, and (C) CTS-CA-II.

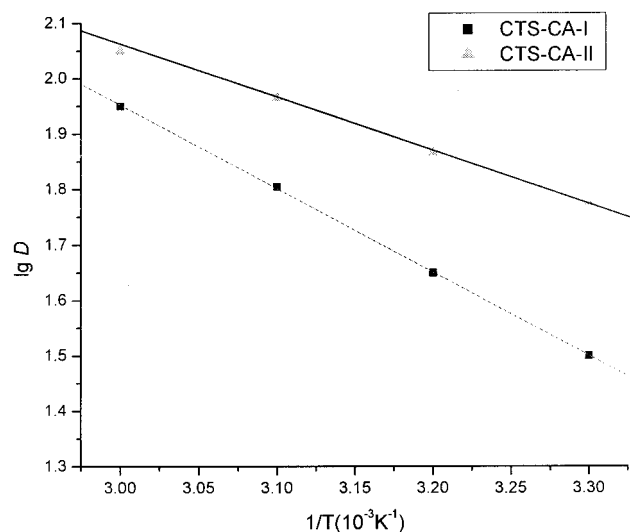


**Figure 7** Effect of temperature on distribution ratio (2 h,  $C_0 = 0.5 \text{ mmol mL}^{-1}$ ).

for  $\text{Ni}^{2+}$ ,  $\text{Cd}^{2+}$ ,  $\text{Cu}^{2+}$ ,  $\text{Pd}^{2+}$ ,  $\text{Ag}^+$ , and  $\text{Hg}^{2+}$  is lower than that of CTS-NH<sub>2</sub> because of both the decrease of nitrogen content and the increase of steric hindrance in CTS-CA. However, the selectivity is different, especially, for the adsorption capacity towards  $\text{Ag}^+$  and  $\text{Hg}^{2+}$ . It is also evident that the adsorption capacity of CTS-CA-II for  $\text{Pd}^{2+}$ ,  $\text{Ag}^+$ , and  $\text{Hg}^{2+}$  is higher than that of CTS-CA-I, possibly because CTS-CA-II has the cavity of an electron-rich benzene  $\pi$ -system in which heavy metal ions can be easily included. In addition, the adsorption capacities of CTS-CA-I and CTS-CA-II for  $\text{Ag}^+$  and  $\text{Pd}^{2+}$  are much higher than those for  $\text{Cd}^{2+}$  and  $\text{Cu}^{2+}$  because of the presence of the calixarene moiety in CTS-CA-I and CTS-CA-II.

#### Effect of temperature

The adsorption capacity of two CTS-CA derivatives for bivalent Hg ion was determined in the temperature range 30–60°C. The results of plotting  $1/T$  versus  $\log D$  (where  $D$  is the distribution ratio:  $D = Q/C$ ) are plotted in Figure 7. The results show that the distribution ratio increases with the increase of the solution temperature, indicating that the adsorption process is both endothermal and chemical. A possible causes of the increase in the distribution ratio are the coincident enhancements of the swelling ability of CTS-CA and

ionic diffusion velocity in aqueous solution with the increase of the solution temperature.

The linear slopes for CTS-CA-I and CTS-CA-II in Figure 7 are  $-1.505 \times 10^3$  and  $-0.925 \times 10^3$ , respectively, and the correlation coefficients ( $r$ ) are both 0.999. According to the relation  $\log D = -\Delta H/2.303RT + C$ ,  $\Delta H$  for CTS-CA-I and CTS-CA-II is calculated as 28.82 and 17.71 kJ/mol, respectively.

#### Effect of acidity of medium on adsorption properties of CTS-CA-I

The experimental results of the effect of acidity of medium on adsorption properties of CTS-CA-I are shown in Table III. The acidity of the medium affected the adsorption properties of CTS-CA-I and CTS-CA-II towards  $\text{Ag}^+$  and  $\text{Cu}^{2+}$  more than those towards  $\text{Pd}^{2+}$  and  $\text{Hg}^{2+}$ . The adsorption capacity of CTS-CA-I for  $\text{Ag}^+$  increased with the pH and that for  $\text{Cu}^{2+}$  decreased with the pH. The adsorption capacities of CTS-CA-I and CTS-CA-II towards  $\text{Pd}^{2+}$  and  $\text{Hg}^{2+}$  remained almost unchanged in the pH range 4.0–7.0.

#### Adsorption kinetics

The dynamic adsorption curves of CTS-CA-I towards  $\text{Ag}^+$  and  $\text{Hg}^{2+}$  are shown in Figure 8a. It is evident that the adsorption velocity of CTS-CA-I toward  $\text{Ag}^+$  is larger than that toward  $\text{Hg}^{2+}$ ; that is, the adsorption of  $\text{Ag}^+$  reaches a plateau within 1 h, whereas the adsorption of  $\text{Hg}^{2+}$  takes 4 h to reach a plateau. The dynamic adsorption curves of CTS-CA-I I towards  $\text{Ag}^+$  and  $\text{Hg}^{2+}$ , shown in Figure 8b, show similar adsorption phenomena for CTS-CA-II. The adsorption velocity of CTS-CA-II toward  $\text{Ag}^+$  is larger than that toward  $\text{Hg}^{2+}$ ; that is, adsorption of  $\text{Ag}^+$  reaches a plateau within half an hour, whereas the adsorption of  $\text{Hg}^{2+}$  takes 3 h to reach a plateau.

#### CONCLUSIONS

CTS-CA derivatives were synthesized by an alkylation reaction of amino or hydroxyl groups on C<sub>6</sub> in CTS with chloroalkyl-substituted calixarenes. The structures of these derivatives were characterized by IR, WAXD, and SEM analyses. The adsorption properties of CTS-CA were determined. Owing to the presence of calixarene moiety The adsorption properties of

**TABLE III**  
Influence of pH on Adsorption Ability of CTS-CA (to CTS-CA-I)

Parameter	$\text{Cu}^{2+}$			$\text{Pd}^{2+}$			$\text{Ag}^+$			$\text{Hg}^{2+}$		
pH	4.0	5.0	7.0	4.0	5.0	7.0	4.0	5.0	7.0	4.0	5.0	7.0
Absorbtion yield (%)	60.8	38.0	20.3	75.0	76.1	78.3	46.7	78.5	85.2	58.3	63.8	55.4

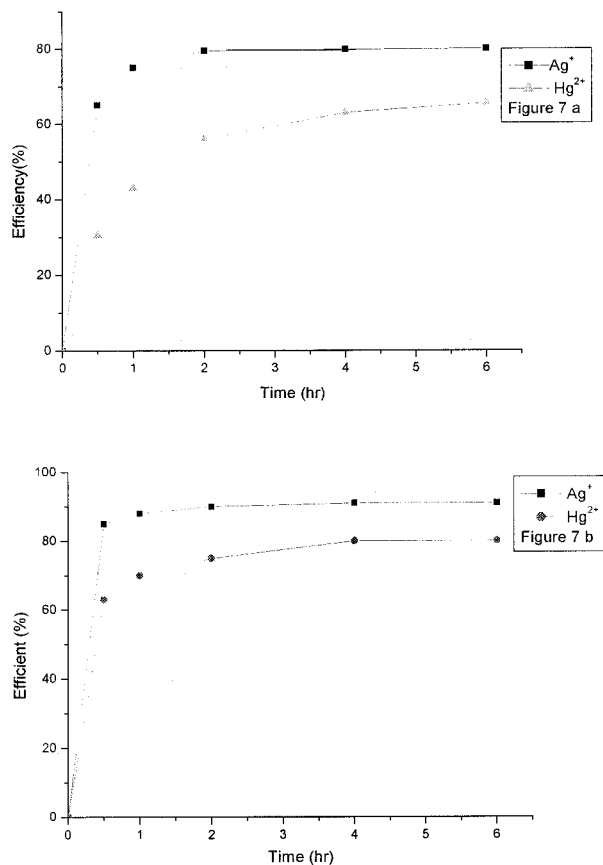


**Figure 8** Adsorption kinetic curves of (a) CTS-CA-I and (b) CTS-CA-II towards  $\text{Ag}^+$  and  $\text{Hg}^{2+}$  at pH 5.0.

CTS-CA-I and CTS-CA-II towards metal ions were very different than those of CTS-NH<sub>2</sub> because of the introduction of the calixarene moiety. The derivatives did not dissolve in general organic solvent and can easily be powdered, thus making them easier to use as adsorbents than CTS.

## References

1. Majeti, N.V.; Ravi, K. *React Funct Polym* 2000, 46, 1.
2. Inoue, K.; Yoshizuki, K.; Ohto, K. *Anal Chim Acta* 1999, 388, 209.
3. Aly, A.S.; Jeon, B.D.; Park, Y.H. *J Appl Polym Sci* 1997, 65, 1939.
4. Peng, C.H.; Wang, Y.T.; Tang, Y.R. *J Appl Polym Sci* 1998, 70, 501.
5. Sashiwa, H.; Shigemasa, Y.; Roy, R. *Macromolecules* 2001, 34, 3905.
6. Yang, Z.K.; Wang, Y.T.; Tang, Y.R. *J Appl Polym Sci* 2000, 77, 3053.
7. Tojima, T.; Katsura, H.; Han, S.-M.; Tanida, F.; Nishi, N.; Tokura, S.; Sakairi, N. *J Polym Sci, Part A: Polym Chem* 1998, 36, 1965.
8. Kurauchi, Y.; Ono, H.; Wang, B.; Egashira, N.; Ohga, K. *Anal Sci* 1997, 13, 47.
9. (a) Gutsche, C.D. *Calixarenes Revisited*; The Royal Society of Chemistry: Cambridge, 1998; (b) *Topics in Inclusion Science: Calixarene, a Versatile Class of Macrocyclic Compounds*; Vicens, J.; Boehmer, V., Eds.; Kluwer: Dordrecht, 1990; (c) Boehmer, V. *Angew Chem Int Ed Engl* 1995, 34, 713.
10. Yang, F.F.; Chen, Y.Y. *Supramol Chem* 2001, 12, 445-448.
11. Chen, Y.Y.; Li, H.B. *New J Chem* 2001, 25, 340.
12. Zhu, B.R.; Shi, Z.Q.; He, B.L. *Ion Exchange Adsorp* 1997, 13, 43.